Beam Diagnostics with Synchrotron Radiation in Light Sources

S. Takano
JASRI / SPring-8

IPAC'10
The 1st International Particle Accelerator Conference

Outline

- Transverse Beam Profiling
- Bunch Length Measurement
- Single Bunch Purity Measurement
- Diagnostics with a Dedicated Insertion Device

Transverse Beam Profiling

Key Instrumentation for Emittance Diagnostics.

$$\varepsilon_i = \frac{\sigma_i^{\,2} - \left(\sigma_E / E\right)^2 \eta_i^{\,2}}{\beta_i} \qquad i = x, y$$

Light Sources are Competing to Achieve

Lower Emittance and Emittance Coupling Ratio.

Vertical Emittance ε_y Approaching to 1 pm rad

$$\varepsilon_y = 1pm \bullet rad, \quad \beta_y \sim 10m \quad \Rightarrow \quad \sigma_y = \sqrt{\varepsilon_y \beta_y} \sim 3\mu m$$

High Resolution is Demanded for Beam Profiling.

List of Transverse Beam Profiling Instruments in Light Sources

	Energy (GeV)	ε_x (nm rad)	ε_y (pm rad)	σ_y (μm)	$\Delta\sigma_y$ (μm)	X-ray	Visible/UV	Reference
SPring-8	8	3.4	7.2	14.1	4.1 -	Zone Plate	 2-dim. inter.	NIMA '06 J.Sync.Rad. '03
PF	2.5	35.5	244	42.2	-		1-dim. inter.	Act. Rep. 2007
UVSOR-II	0.75	27.4	<274	<80	-		1-dim. inter.	-
TLS	1.5	21.5	55.5	30	-		1-dim. inter.	PAC '05
SSRF	3.5	3.9	47	34	10 -	Pinhole	 1-dim. inter.	- DIPAC '09
ASP	3	10.4	4.5	~20	~65	Pinhole		EPAC '08
ESRF	6	3.7	7	16	3.5 -	Pinhole In air X-ray		- DIPAC'07
SLS	2.4	5.6	3.2	6.4	- 9	 Pinhole	π-polarization	NIMA '08 DIPAC '07
BESSY II	1.7	5.2	<100	40	3 11	BF lens Pinhole		NIMA '01 NIMA '01
MAX II	1.5	9		30	-		π-polarization	EPAC '06
ANKA	2.5	50		34	-	In air X-ray		EPAC '06
SOLEIL	2.75	3.7	3.7	< 8.4	~5	Pinhole		DIPAC '07
Diamond	3	2.7	1.7	5.9	3.4	Pinhole		PRSTAB'10
ALBA	3	4.3	43	32	~15	Pinhole		EPAC '06
PETRA III	6	1	10	18.5	1~2 16	CR lens Pinhole		IPAC'10 IPAC'10
APS	7	2.5	40	-	~12	Pinhole		EPAC '98
ALS	1.9	6.3	~5	~10	- 33	K-B mirror Pinhole		R. Sci. Instr.'96 EPAC '04
SPEAR3	3	10	<10	20	>10 -	Pinhole	 1-dim. inter.	EPAC '06 PAC '09
CLS	2.9	18	~30	~30	~11	Pinhole		NIMA'08
NSLS-II	3	0.5 - 2	8	12	2 9	CR lens Pinhole		- PAC'09

Trends in Modern Light Sources

X-ray pinhole cameras and visible SR interferometers are widely used.

Developments of imaging systems based on the X-ray focusing optics are pursued to further improve the spatial resolution.

Other Methods are also performing such as π-polarization method and in-air X-ray monitors.

X-ray Pinhole Camera

System Resolution

$$\boxed{\Delta\sigma_y{}^2 = S_{Pinhole}{}^2 + S_{Camera}{}^2}$$

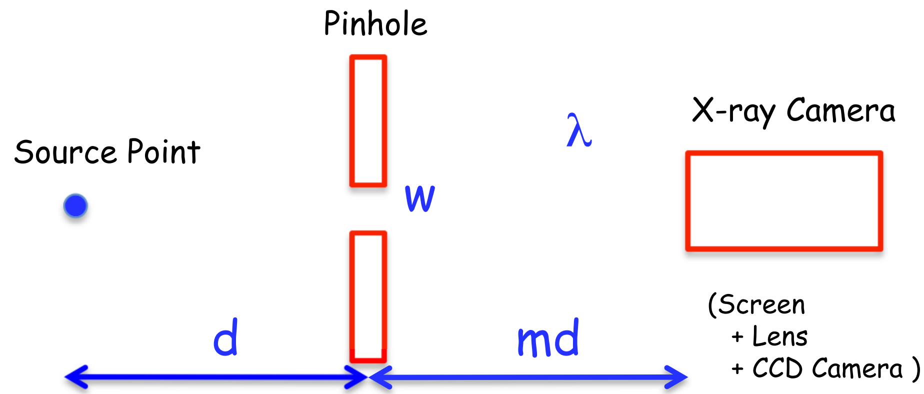

Pinhole Optimization

Simplistic Model

$$S_{Pinhole}{}^2 = S_{Diffraction}{}^2 + S_{Aperture}{}^2 \qquad S_{Diffraction} = \frac{0.36\lambda d}{w}, \qquad S_{Aperture} = \frac{w(1+1/m)}{\sqrt{12}}$$

Given d, m, and λ $\boxed{S_{Pinhole\_opt} = 0.46\sqrt{\lambda d\left(1+\frac{1}{m}\right)}}$ with $w_{opt} = 1.12\sqrt{\frac{\lambda d}{1+1/m}}$

For better resolution...

closer distance d, larger magnification m,

and shorter observing wavelength λ.

X-ray Pinhole Camera

Quantitative optimization
needs PSF calculation
based on wave optics
taking account of
the SR bandwidth.

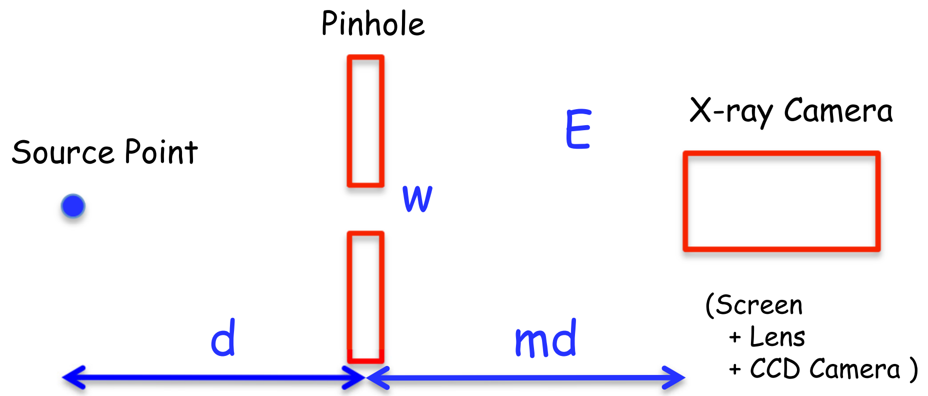

	d (m)	m	w (μm)	E_{Peak} (keV)	Simple Model $S_{pinhole}$ (μm) @ E_{Peak}	Wave Optics $S_{pinhole}$ (μm)	Reference
SOLEIL	4.36	1.3	10	~60	6.0	3.6	DIPAC'07
Diamond P2	4.45	2.7	25	26	10.4	2.6	PRSTAB'10

The most performing X-ray pinhole cameras are elaborately designed to achieve resolution in the μm range.

X-ray Pinhole Camera @ SOLEIL

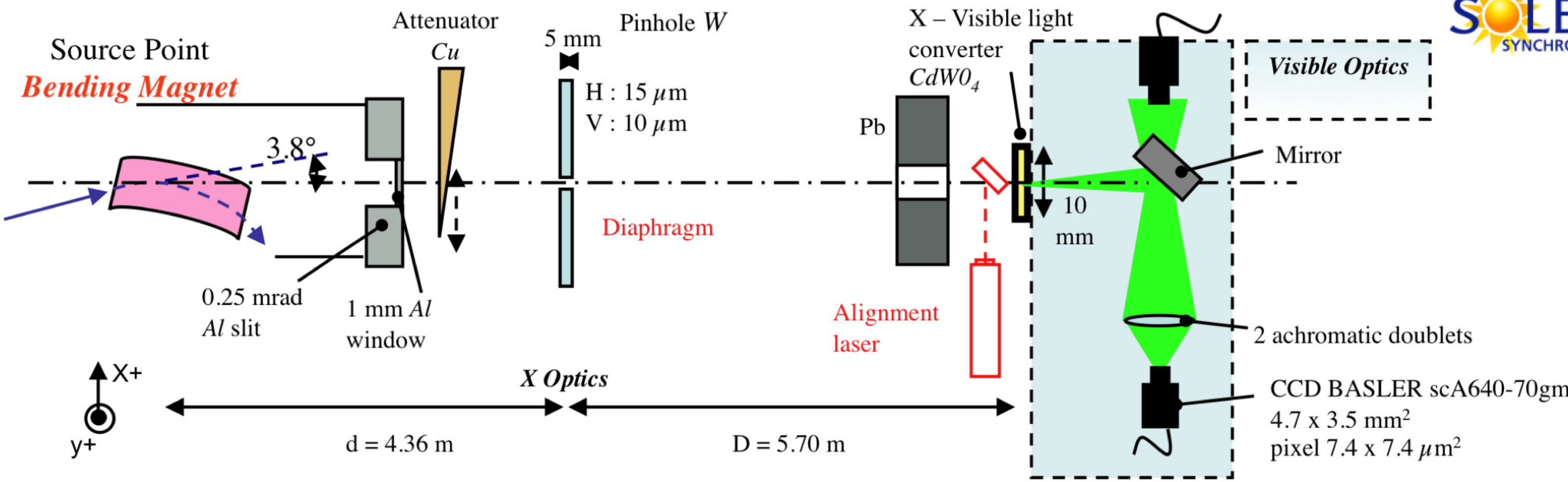

Minimum Coupling

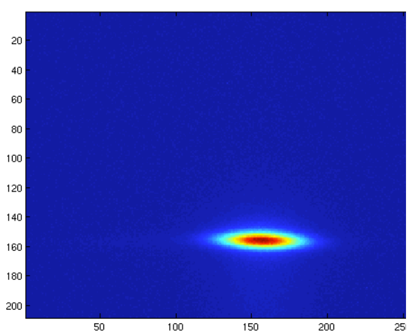

K < 0.1%
$\varepsilon_V \cong 3.5$ pm

Pinhole
$w = 10\ \mu m$
$S_{Pinhole} = 3.6\ \mu m$

Visible Optics
$S_{Camera} = 2\ \mu m$

- Pinhole design from ESRF
- The resolution analysis is a SOLEIL work
- Beam-based pinhole aperture measurements in progress to control if the theoretical pinhole size is really set.

System Resolution
$\Delta\sigma_y = 4.1\ \mu m$

Courtesy of M.-A. Tordeux and J.-C. Denard, SOLEIL

Pioneering Works with X-ray Imaging Optics

Kirkpatrick-Baez Mirror (K-B mirror)

ALS, PLS

K-B mirror@ALS
Renner et al.
Rev. Sci. Instrum. 67, 3368 (1996).

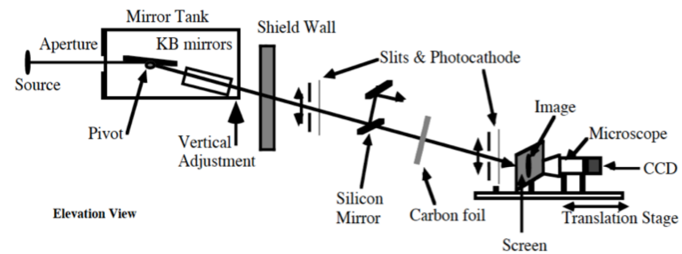

Bragg-Fresnel Lens (BFL)

ESRF, BESSY II

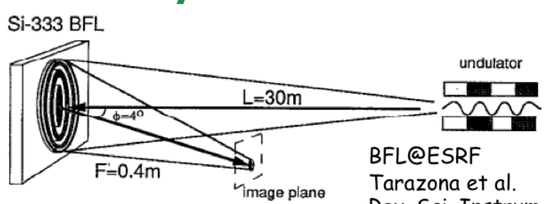

BFL@ESRF
Tarazona et al.
Rev. Sci. Instrum. 65, 1959 (1995).

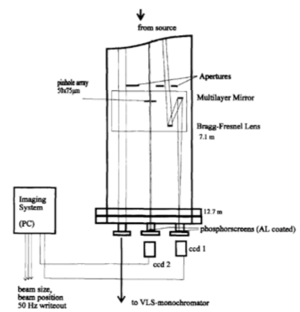

BFL@BESSY II
Holldack et al.
N.I.M.A. 365, 40 (1995).

Fresnel Zone Plate (FZP)

APS

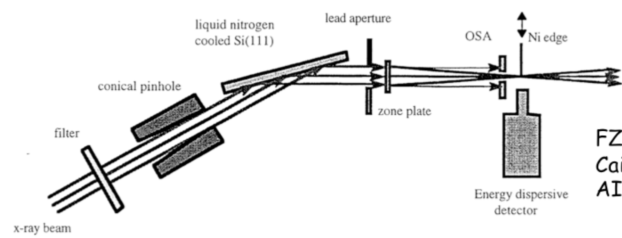

FZP@APS
Cai et al.
AIP CP417, 101 (1995).

Compound Refractive Lens (CRL)

ESRF

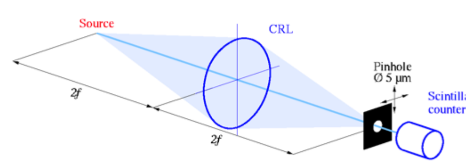

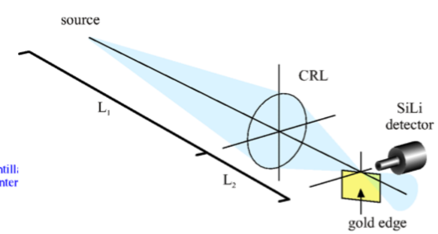

CRL@ESRF
Weitkamp et al.
EPAC'00, 1824 (2000).

Beam Profiling with X-ray Imaging Optics

Developments of imaging systems based on the X-ray focusing optics are pursued to further improve the spatial resolution.

Compound Refractive Lens (CRL)

- PETRA III
- NSLS-II (planned)

Fresnel Zone Plate (FZP)

- SPring-8

CRL Optics @ PETRA III

Compound Refractive Lens

lens-maker formula: $1/f = 2(n-1) / R$

X-ray refraction index : $n = 1 - \delta + i\beta, \quad \delta \approx 10^{-6}$

- concave lens shape
- strong surface bending R

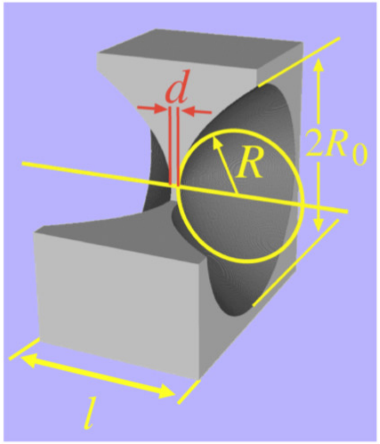

- small Z (Be, Al, …)
- small d

$$\boxed{f = \frac{R}{2\delta N}} \Longrightarrow \text{many lenses (N=10…300)}$$

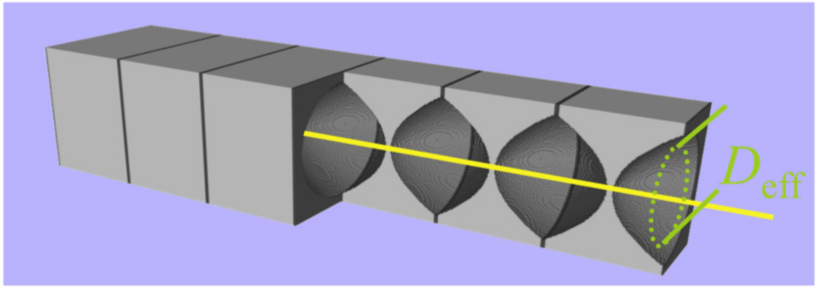

PETRA III @ 20 keV:

- $R = 200$ µm, $R_0 = 500$ µm, $d = 10$ µm, $l = 1$mm
- $N = 31$
- material: beryllium

$f = 3.72$ m

Courtesy of G. Kube, PETRA III

Diagnostics Beamline with CRL System @ PETRA III

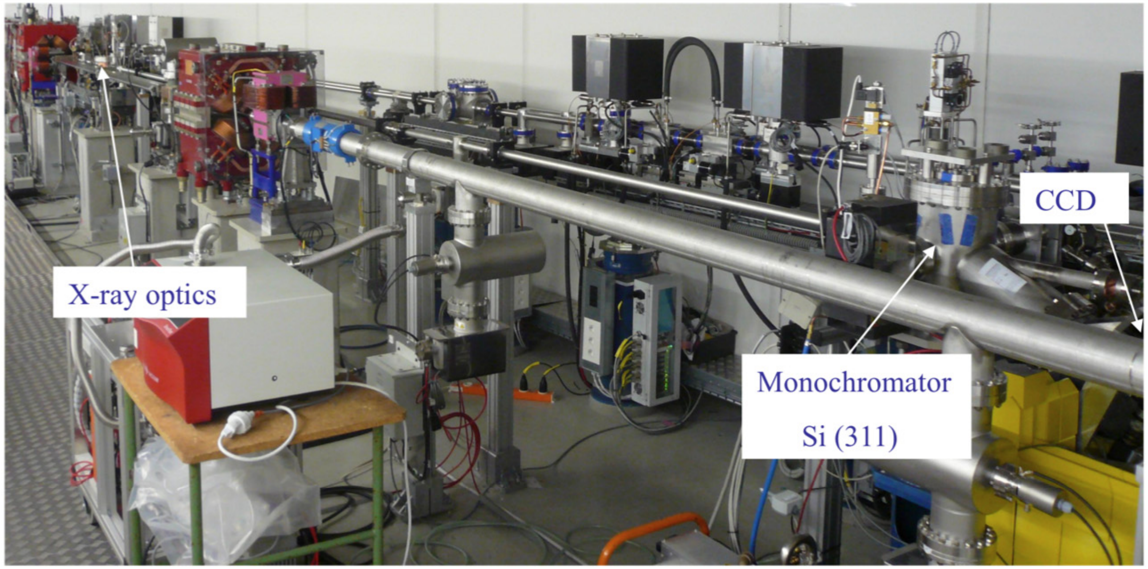

CRL f = 3.72 m @ 20 keV
magnification ~ 1.55
σ_{CRL} ~ 0.2 μm

X-ray Detector System
σ_{Camera} ~ 6 μm curently
σ_{Camera} = 1~2 μm
in preparation

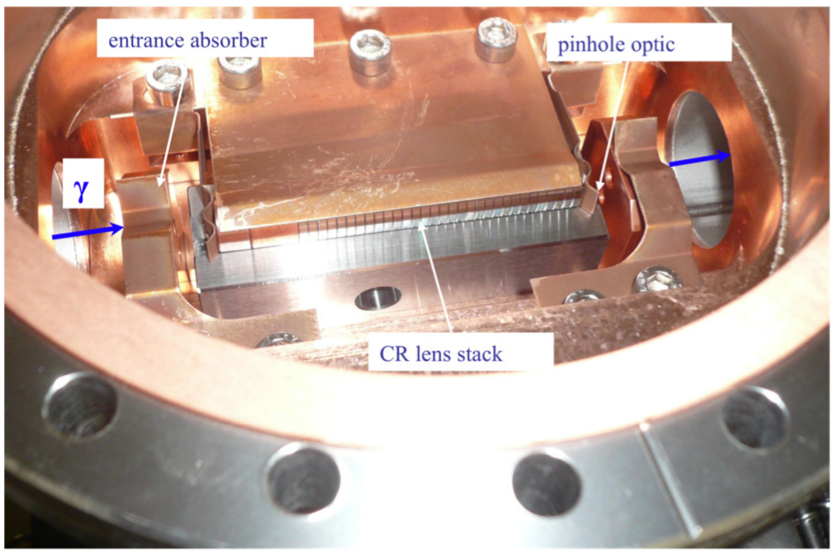

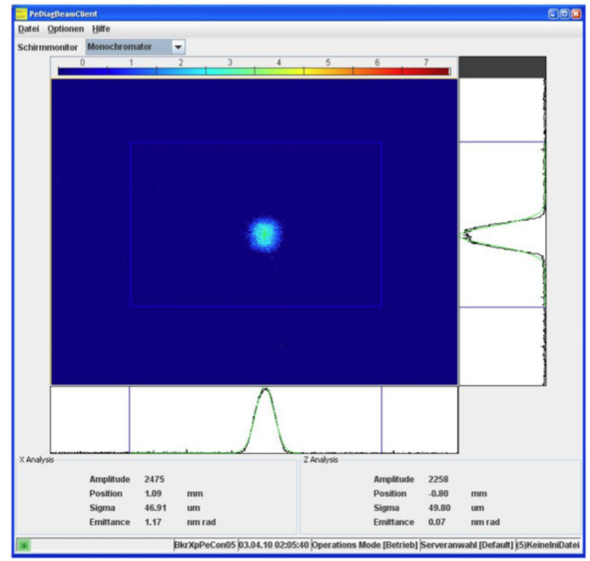

Courtesy of
G. Kube,
PETRA III

Details given in
IPAC'10 Poster
MOPD089
" PETRA III Diagnostics Beamline
for Emittance Measurements"

Fresnel Zone Plate (FZP) Optics

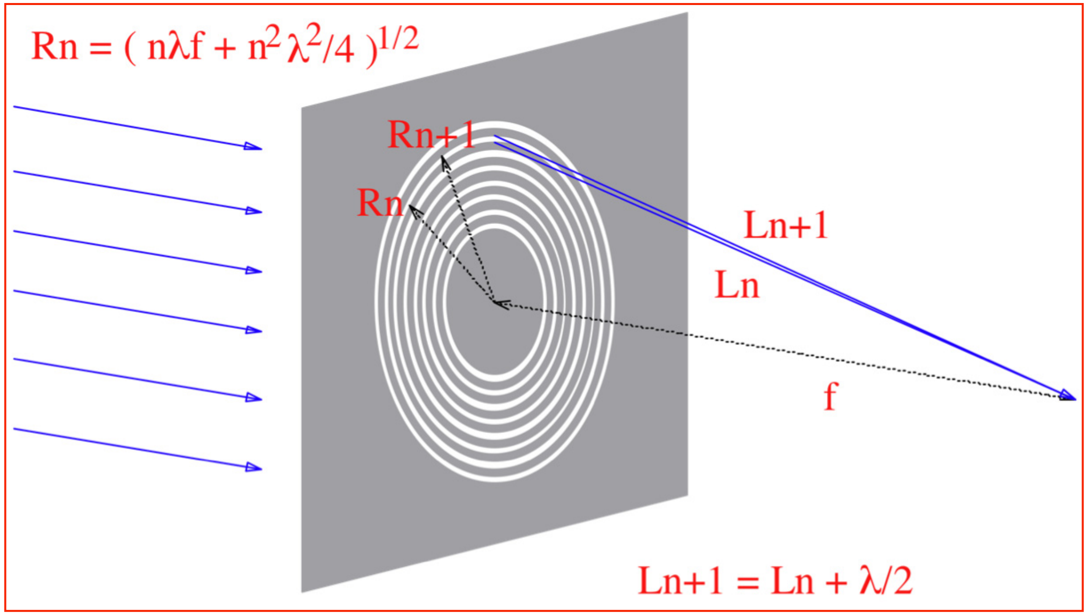

Between rays passing adjacent transparent zones,
The difference of optical paths to a focal spot is equal to one wavelength.

The rays passing all the transparent zones contribute in phase at a focal spot to the amplitude.

In the hard X-ray region, absorbing zones are not completely opaque.
If the phase shift originating from absorbing zone material corresponds to the half wavelength,
The rays passing absorbing zones also contribute in phase at a focal point.

X-ray Beam Imager (XBI) @ SPring-8

Single FZP + X-ray Zooming Tube

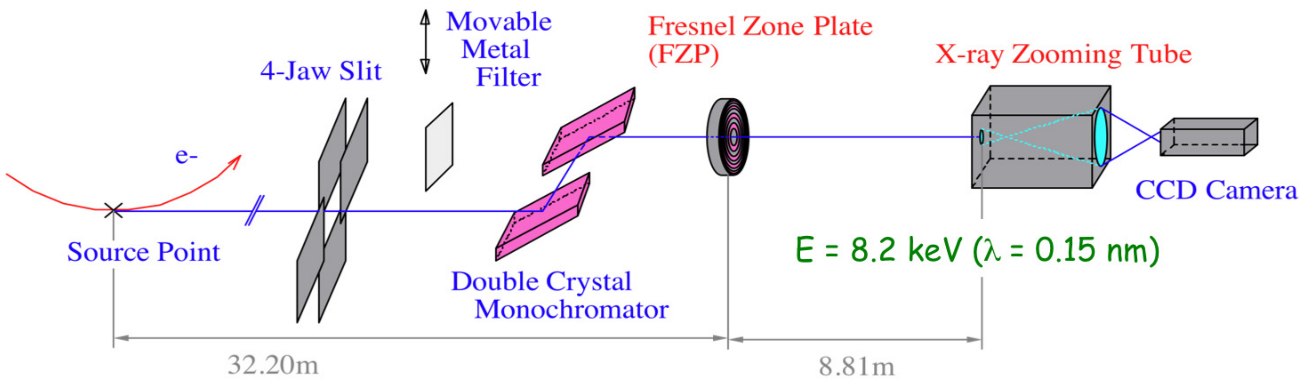

System Resolution	4.1 μm
Time Resolution	1 ms
Field of View	≥ ϕ 1.5 mm
Magnification	13.7

FZP

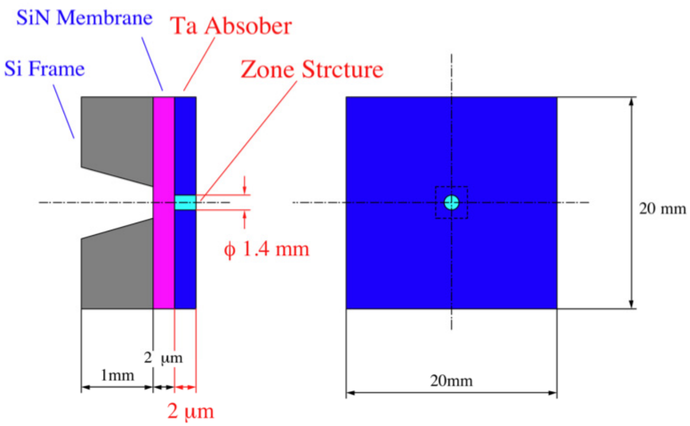

Focal length f	6.92 m
Magnification factor	0.274
Resolution σ_{FZP}	1.5 μm
Efficiency	32 %
Number of Zones	468
Minimum Zone Width	0.75 μm

Low-emittance User Optics (Regular)
ε = 3.4 nm rad

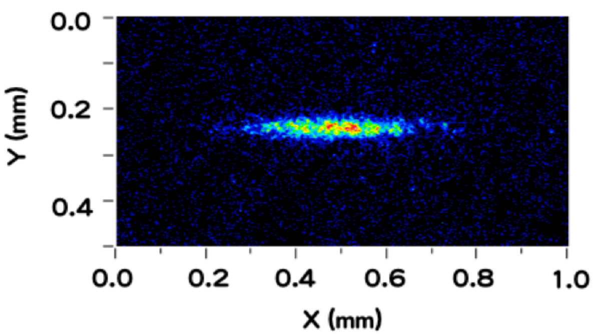

$\sigma_x = 111.7 \pm 1.1$ μm $\sigma_y = 14.1 \pm 0.14$ μm

Synchrotron Radiation (SR) Interferometer

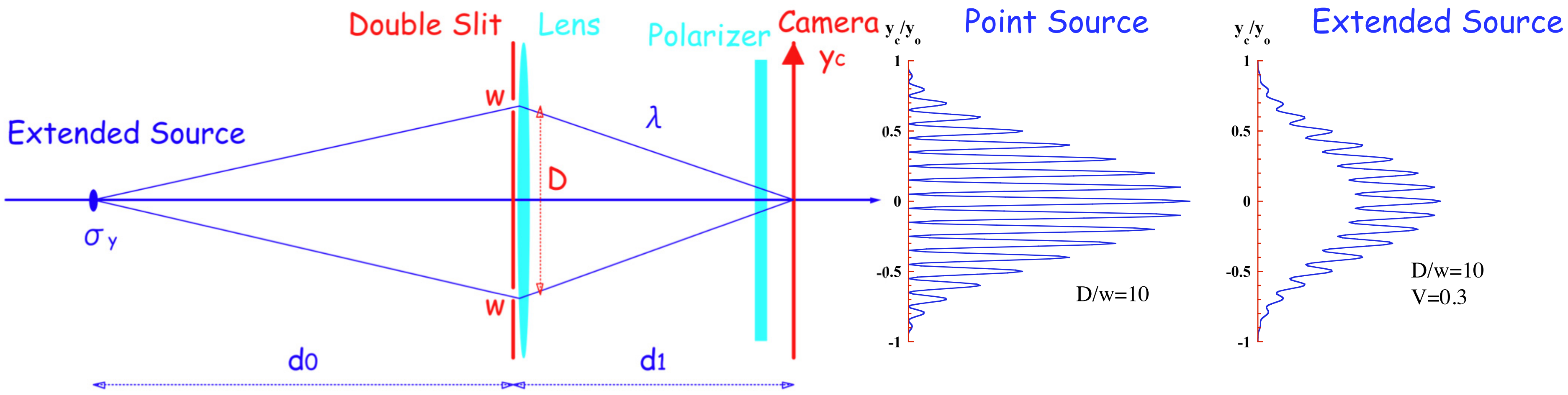

T. Mitsuhashi noted the application of the method to transverse beam profiling.
proc. of PAC'97 (1997) p.766

Interference Pattern

$$I = I_0 \left\{ \mathrm{sinc}\left(\pi \frac{y_c}{y_0} \right) \right\}^2 \left[1 + V \cos\left(2\pi \frac{D}{w} \cdot \frac{y_c}{y_0} \right) \right], \qquad y_0 = \frac{d_1 \lambda}{w}$$

Extended source smears out the interference fringe.

Visiblity

$$V = \frac{I_{\max} - I_{\min}}{I_{\max} + I_{\min}} = \exp\left(-2 \frac{\pi^2 D^2 \sigma_y{}^2}{\lambda^2 d_0{}^2} \right) \Rightarrow \boxed{\sigma_y = \frac{\lambda d_0}{\pi D} \sqrt{\frac{1}{2} \ln\left(\frac{1}{V}\right)}}$$

SR interferometer @ SSRF

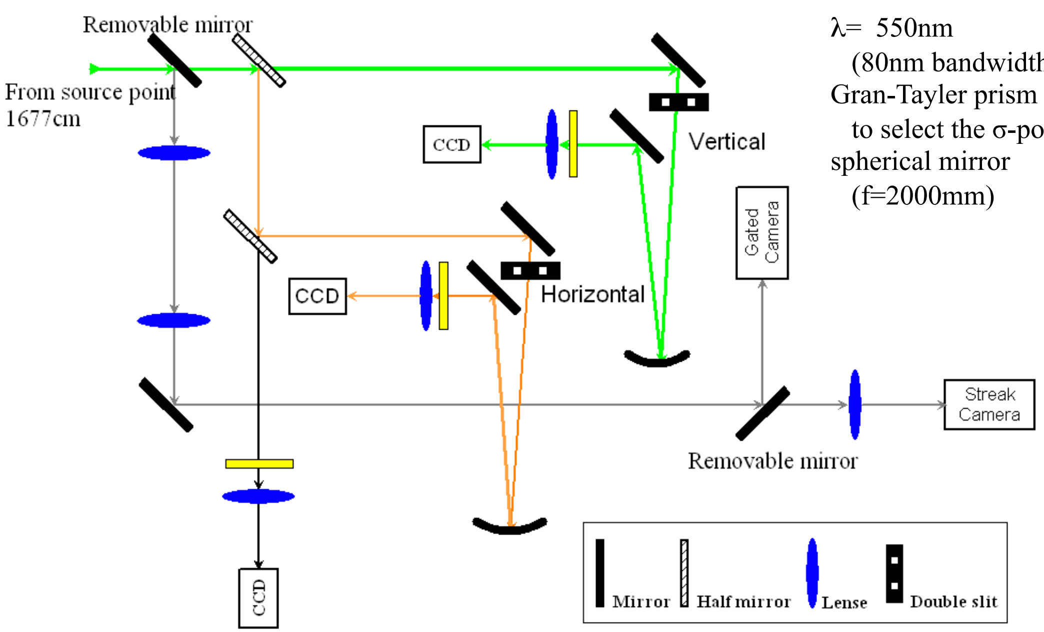

λ= 550nm
(80nm bandwidth)
Gran-Tayler prism
to select the σ-polarization
spherical mirror
(f=2000mm)

First Mirror

- Be
- Parabolic back surface
- two cooling tubes

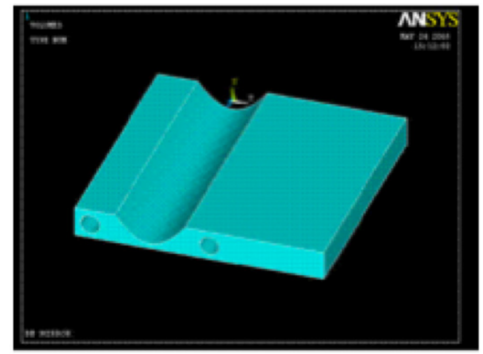

Interferogram

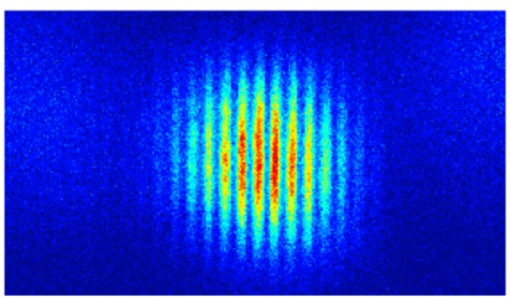

Patten for different current

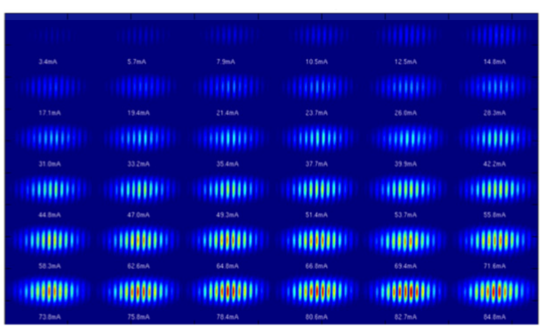

Beam size measurement for transverse feedback

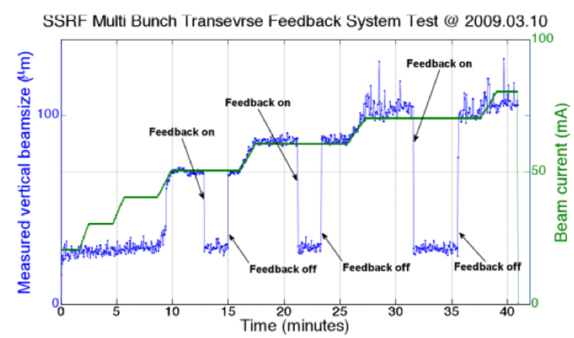

Courtesy of K.R. Ye & Y.B. Leng, SSRF

2-D SR Interferometer @ SPring-8

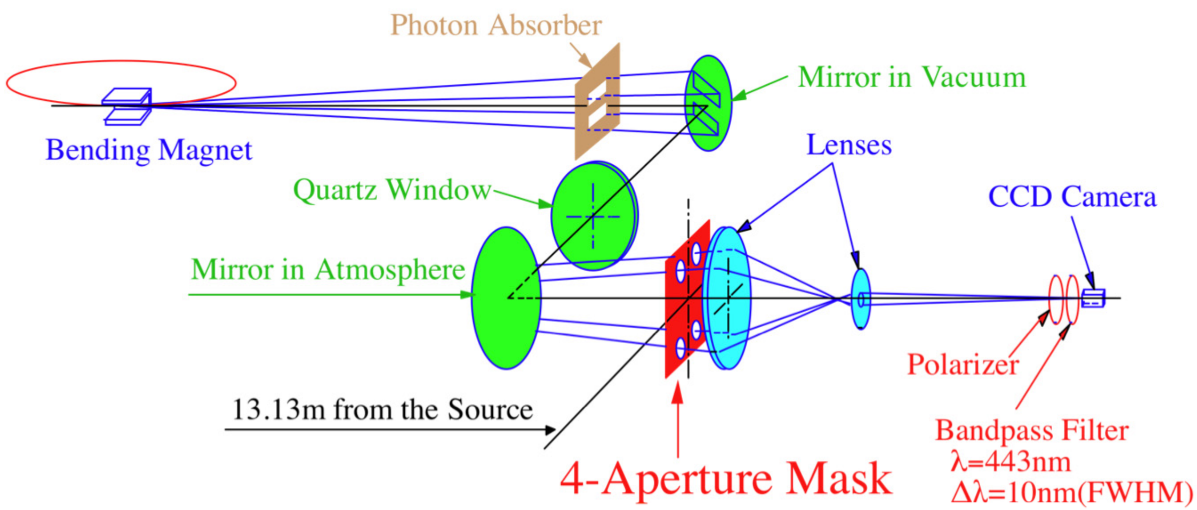

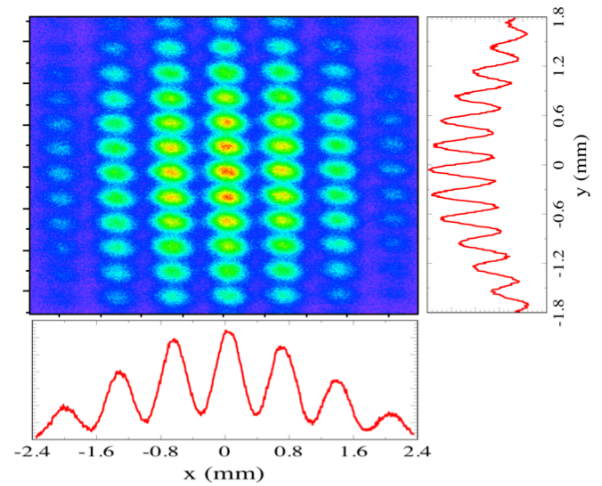

1-D Analysis

$$\sigma_{x,y} = \frac{\lambda}{\pi\eta_{x,y}}\sqrt{-\frac{1}{2}\ln V_{x,y}}$$

V : visibility

λ : observing wavelength

η : angular separation of the 4 - aperture mask

σ : projected rms beam size at the source point

2-D Analysis

$$\tilde{I}(x,y) = \int_{-\infty}^{\infty} I(x,y;x_e,y_e)\rho(x_e,y_e)dx_e dy_e$$

point spread function : $I(x,y;x_e,y_e)$

ellipsoidal electron beam distribution :

$$\rho(x_e,y_e) \propto \exp\left[-\frac{1}{2}\left(ax_e{}^2 + by_e{}^2 + cx_e y_e\right)\right]$$

$$a = \left(\frac{\cos\theta}{\sigma_I}\right)^2 + \left(\frac{\sin\theta}{\sigma_{II}}\right)^2, b = \left(\frac{\sin\theta}{\sigma_I}\right)^2 + \left(\frac{\cos\theta}{\sigma_{II}}\right)^2, c = \left(\frac{1}{\sigma_I{}^2} - \frac{1}{\sigma_{II}{}^2}\right)\sin 2\theta$$

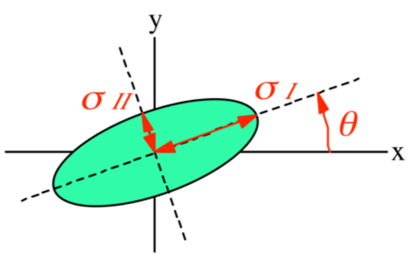

We can obtain the parameters σ_I, σ_{II}, θ by fitting procedure.

Courtesy of M. Masaki, SPring-8

π-Polarization Method

originally developed at MAX II

Imaging with Vertically Polarized Visible-to-UV SR

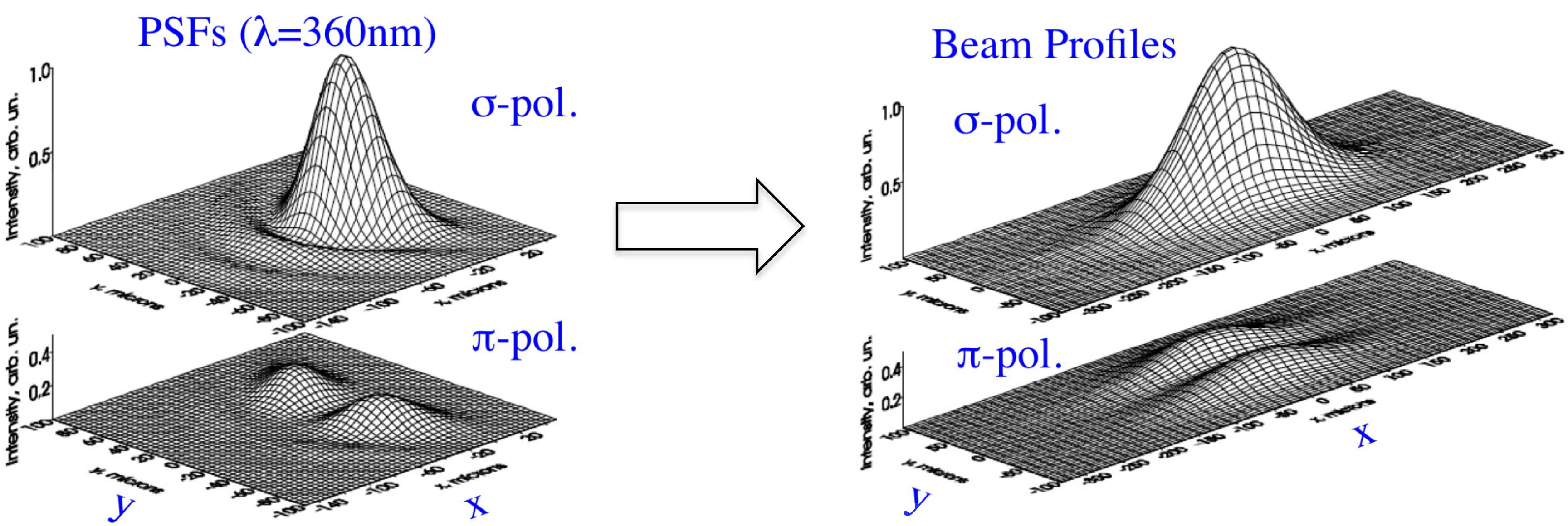

Å.Andersson et al. Proc. EPAC'96(1996) p1689.

Vertical source size σ_y smears out the zero minimum at the center of the π-component PSF.

π-Polarization Method @ SLS

Å.Andersson et al., Nucl. Instr. and Meth. A591 (2008) p.437.

SLS Diagnostic Beamline

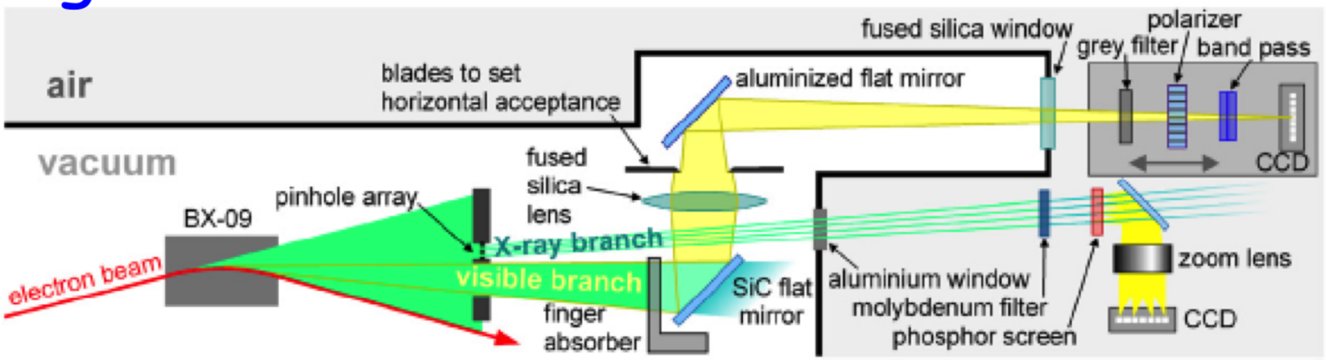

Vertical Profiles

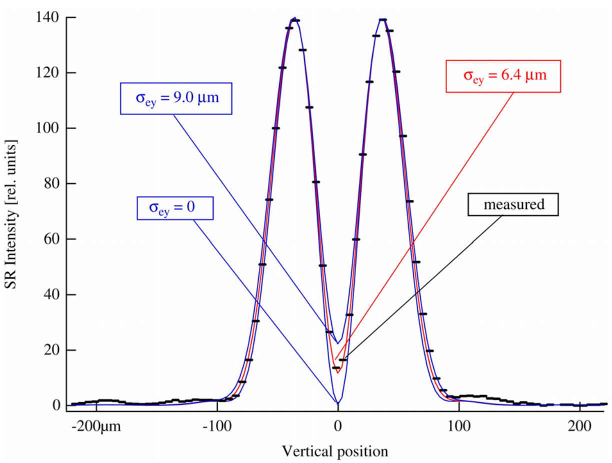

σ_y = 6.4 ± 0.5 µm

Acquired Image

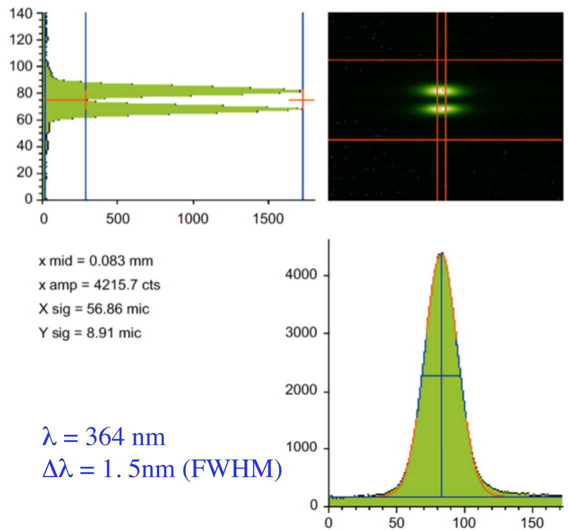

Horizontal Profiles

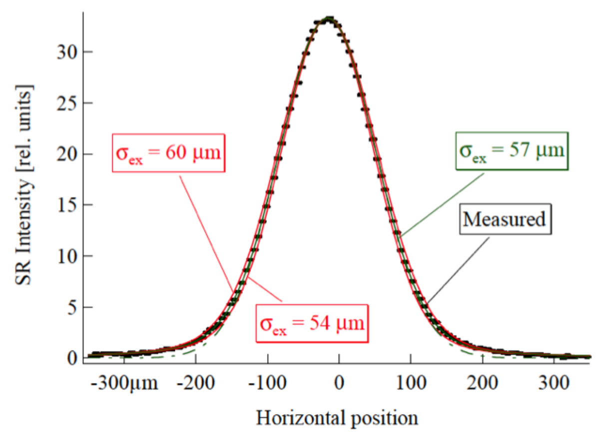

In-Air X-ray (IAX) Monitors @ ESRF

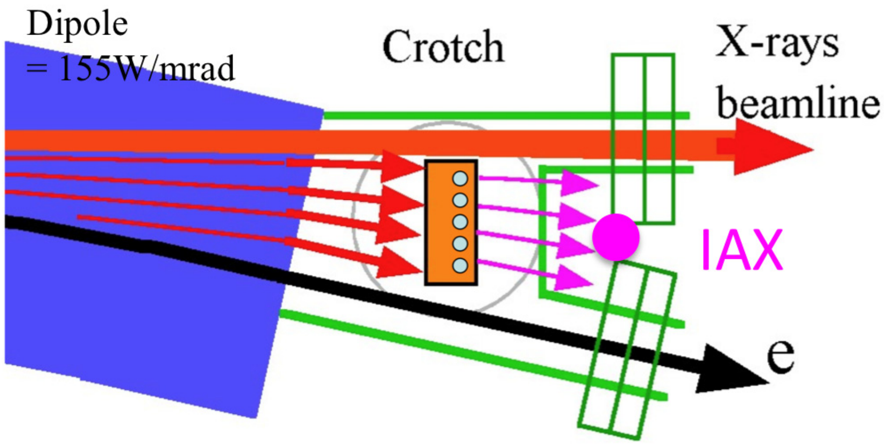

IAX monitors on 11 dipoles (behind crotch absorbers)

a tiny fraction (~2·10^{-6} = 300uW/mrad) traverses the crotch : Xrays > 150KeV

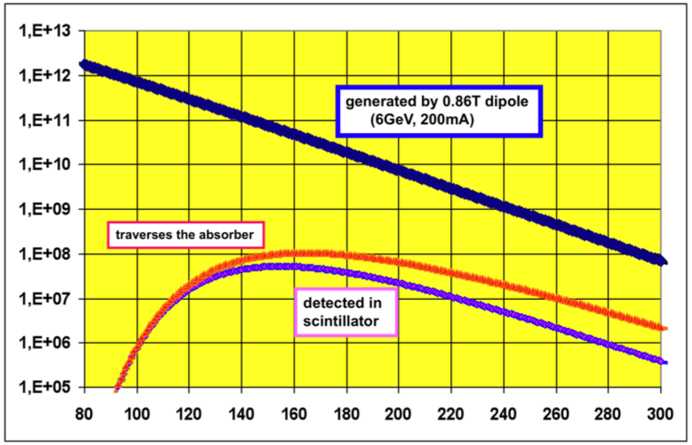

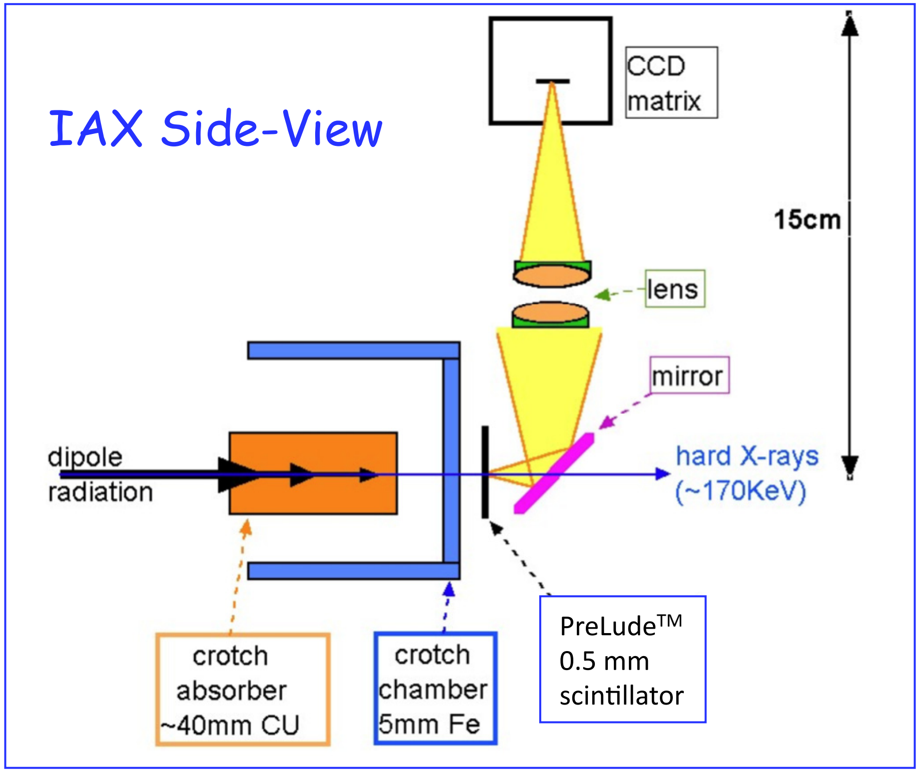

Courtesy of K. Schedt, ESRF

IAX Monitors @ ESRF (Cont')

The projected beam size h
is measured by the IAX.

The source size σ_v can be obtained
by subtracting contribution
of photon beam divergence α_v.

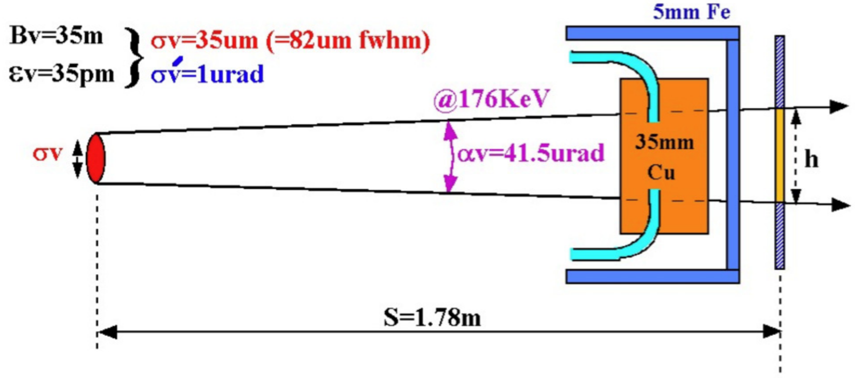

$$h\ [fwhm] = \sqrt{(\sigma v \times 2.35)^2 + S^2 \times (\alpha v^2 + (2.35 \times \sigma v')^2)} = 111um$$

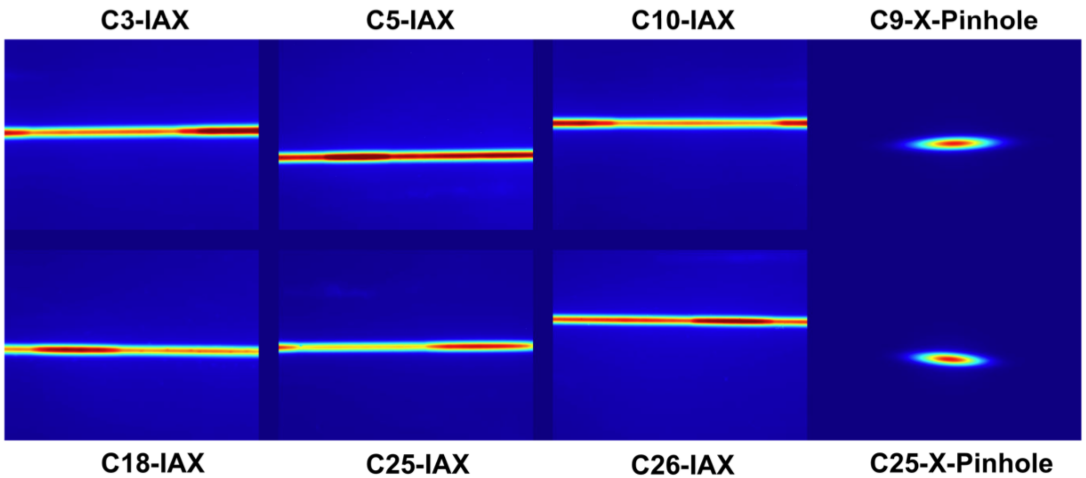

Advantage :
- easy, simple, cheap, compact
- -> can have many of them
- -> useful for local emittance coupling correction

Drawbacks :
- limited resolution & absolute precision for small emittance values (for ε <40pm)
- NO info in horizontal plane

Courtesy of K. Schedt, ESRF

IAX monitors are also used at ANKA.

A.-S. Müller et al., Proc. EPAC06 (2006) p.1073.

Bunch Length Measurement

Topics from Recent Develpoments ...

Fluctuation Analysis

ALS

SR/Laser Cross Correlation

ALS, SPEAR3

Incoherent Radiation Fluctuation Analysis

Based on the method described in Zolotorev, Stupakov, SLAC-PUB 7132 (1996)

In real beams, due to the random modulation in the bunch longitudinal distribution, and to the passage to passage variation of this modulation, incoherent radiation is emitted with intensity and spectrum fluctuating passage to passage.

It has been shown that by measuring the variance of the radiation in intensity in a part of the spectrum where the emission is incoherent, the bunch length can be measured.

Example: synchrotron radiation from a bending magnet

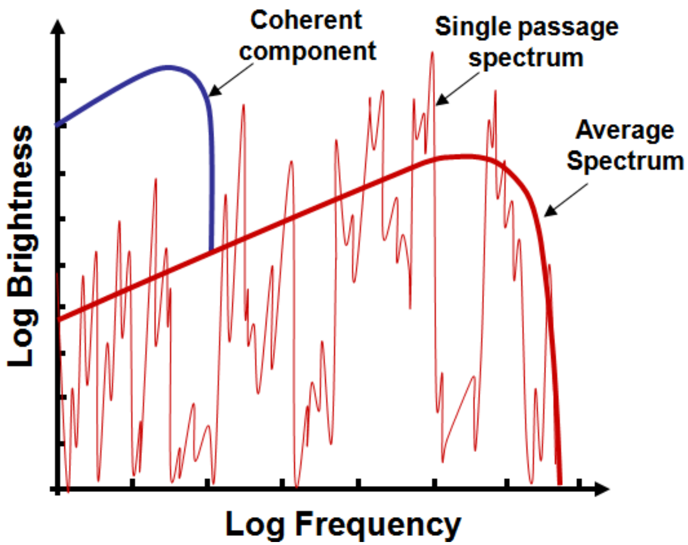

Courtesy of F. Sannibale, ALS

Proof-of-Principle Experiment @ The ATF at BNL

P. Catravas et al., Phys. Rev. Lett. 82, 5261 (1999).

Single-shot specta of spontaneous undulator emission showing fluctuational characteristics measured

Length of a 1-5 ps long bunch successfully extracted

Incoherent Radiation Fluctuation Analysis @ ALS

A simpler scheme with a band-pass filter

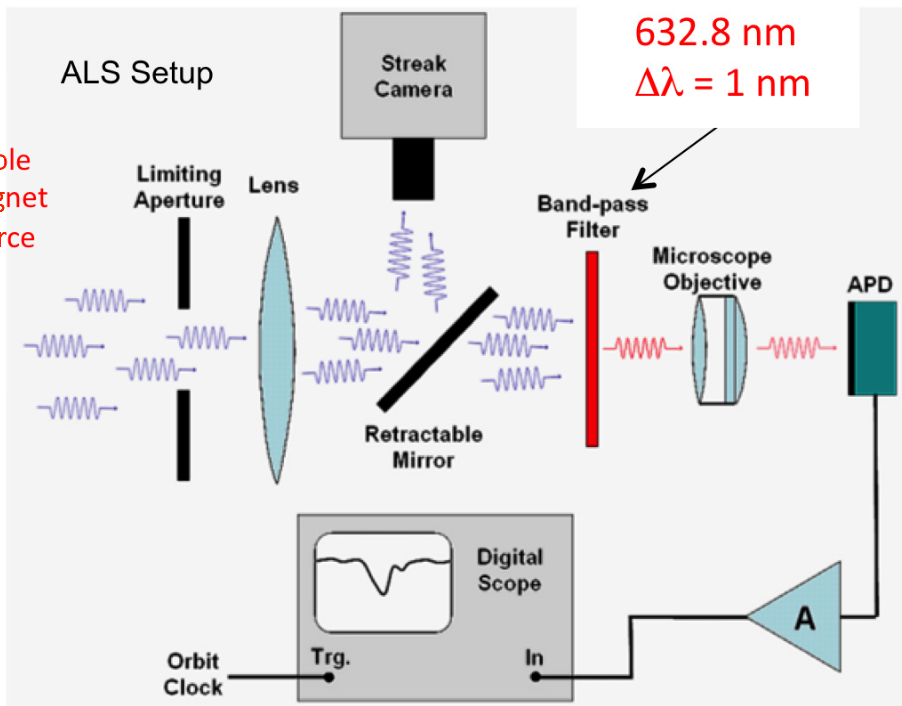

Courtesy of F. Sannibale, ALS
PRST-AB 12, 032801 (2009).

Radiation intensity within a fixed bandwidth $\Delta\lambda$ measured turn-by turn

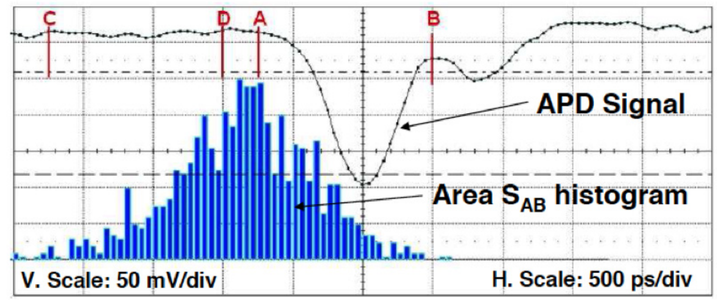

S_{AB}: photon signal including electronic noise
S_{CD}: measure of noise contribution

A complete 5k sample measurement required ~ 1 minute

Intensity Fluctuation

$$\delta_M^{\ 2} = \frac{\sigma_{S_{AB}}^{\ 2} - \sigma_{S_{CD}}^{\ 2}}{\left(\langle S_{AB}\rangle - \langle S_{CD}\rangle\right)^2}$$

Incoherent Radiation Fluctuation @ ALS (cont')

Analysis

$$\delta^2 = {\delta_M}^2 - \frac{s^2}{\langle N_P \rangle}$$

$$\boxed{\frac{s^2}{\langle N_P \rangle}}$$

Photon Shot Noise Contribution

evaluated by performing 2 or more measurements of ${\delta_M}^2$
for the same bunch length
for different number of photons

$$= \frac{1}{\sqrt{1+4{\sigma_\omega}^2{\sigma_t}^2}\sqrt{1+{\sigma_x}^2/{\sigma_{xc}}^2}\sqrt{1+{\sigma_y}^2/{\sigma_{yc}}^2}}$$

$$\cong \frac{1}{\sqrt{1+4{\sigma_\omega}^2{\sigma_t}^2}\sqrt{1+{\sigma_x}^2/{\sigma_{xc}}^2}}$$

σ_t : r.m.s. bunch length
σ_ω : r.m.s. band-width of the filter
σ_{xc}, σ_{yc}: transverse coherence lengths
σ_x, σ_y : transverse beam sizes

Results

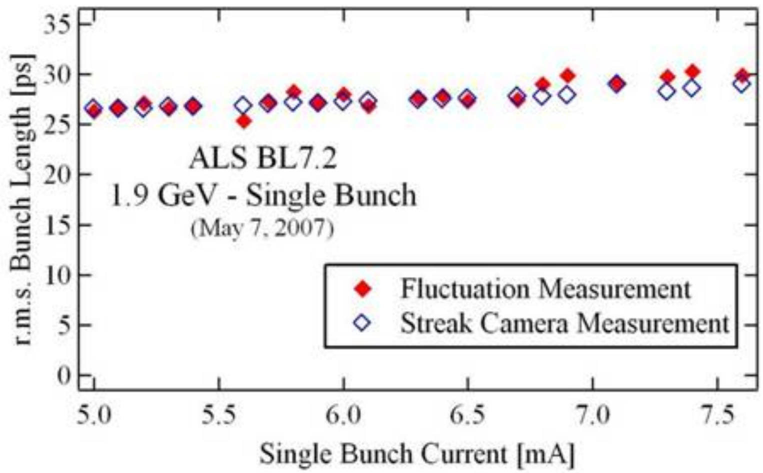

Courtesy of F. Sannibale, ALS
PRST-AB 12, 032801 (2009).

SR/Laser 'Cross-Correlation' Method

proof of principle experiment on ALS (M. Zolotorev et al, PAC'03)

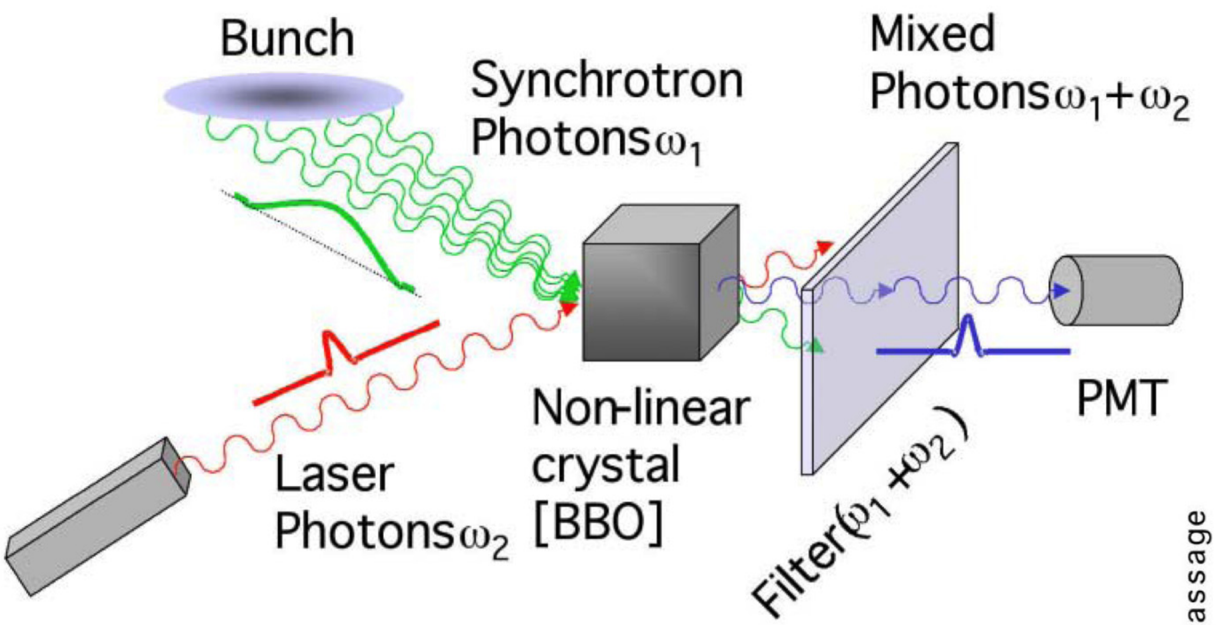

Mixing of SR and Laser in a non-linear crystal

↓

Up-Converted Radiation

Good Time Resolution

↑

Short Laser Pulse Length

Mode Locked TiS Laser Oscillator
- repetition 71 MHz (14 ns)
- pulse length 50 fs
- wavelength 800 nm
- power 100-200 mW
- phase locked to the ring RF

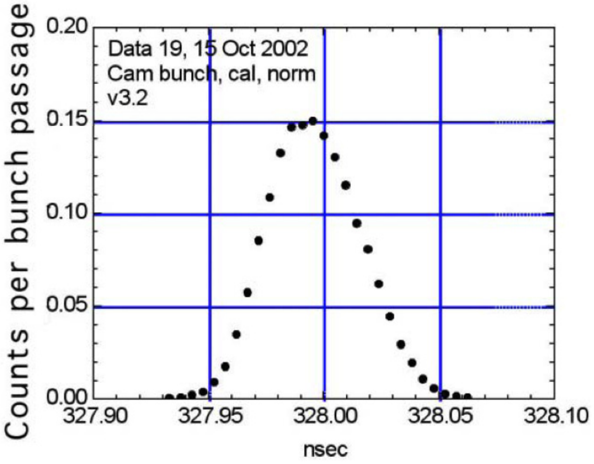

SR/Laser 'Cross-Correlation' Measurement

Experimental Schematic April 2010

@ SPEAR3

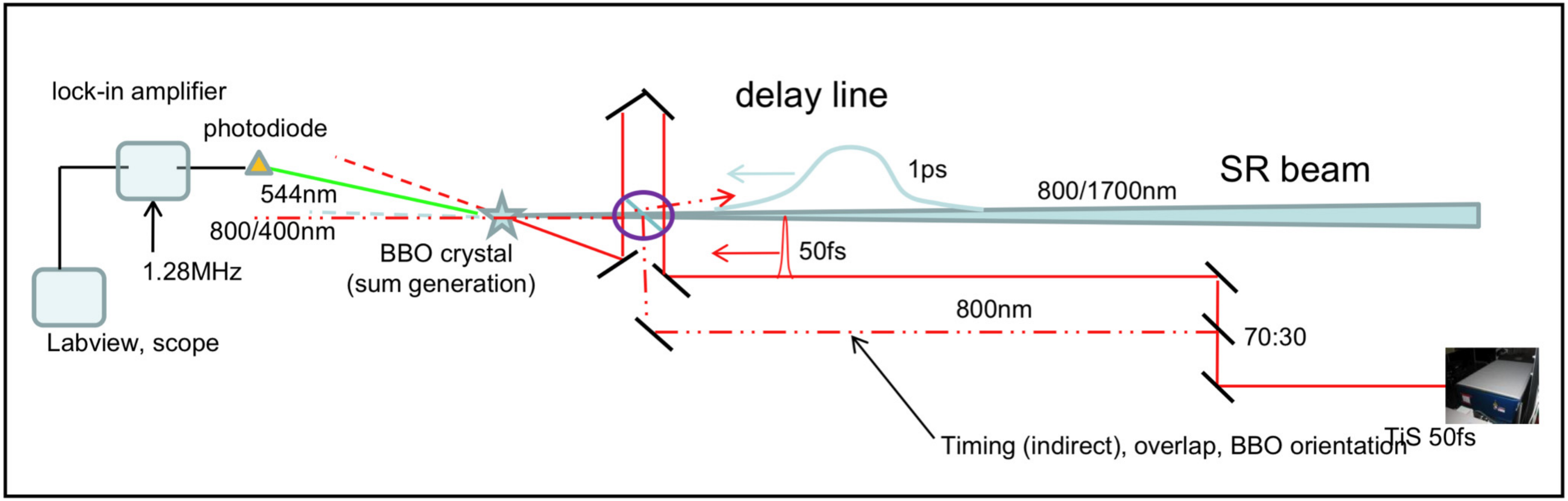

Singnal Detection
- APD
- Lock-in Amplifier
  - 1.28MHz ring frequency

Mode Locked TiS Laser Oscillator
- repetition 5MHz
- pulse length 50 fs
- wavelength 800 nm

April 6, 2010 scan : 15mA single bunch

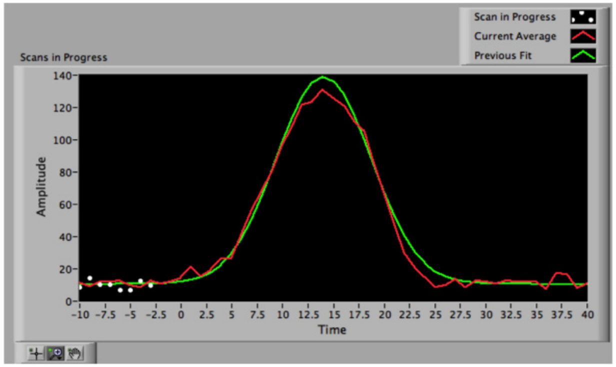

Courtesy of J. Corbett, SPEAR3

Details given in IPAC'10 Contributed Oral WEOCMH03
"Bunch Length Measurements by SR/Laser Cross-Correlation"

Single Bunch Purity Measurement

Time Correlated Single Photon Counting (TCSPC)

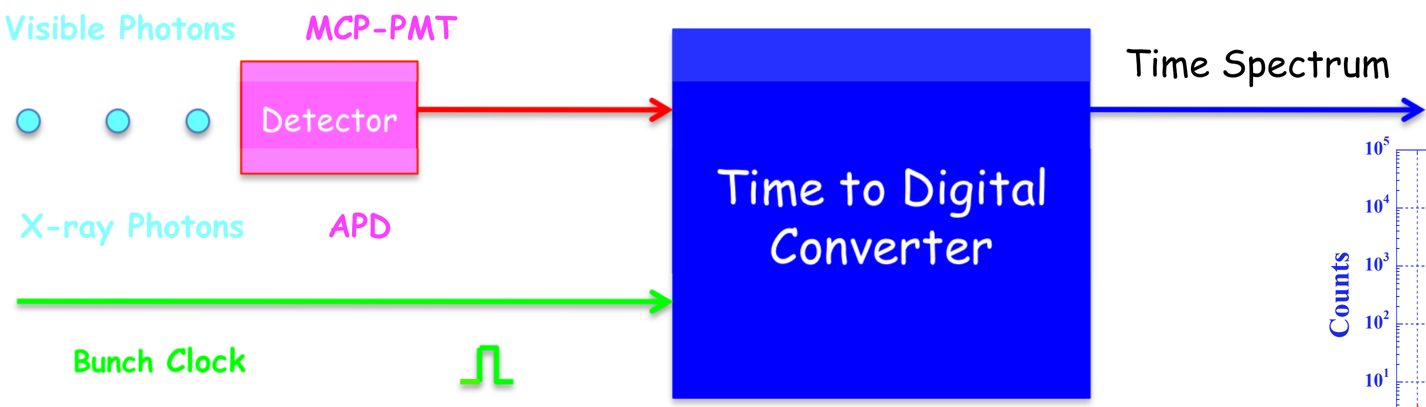

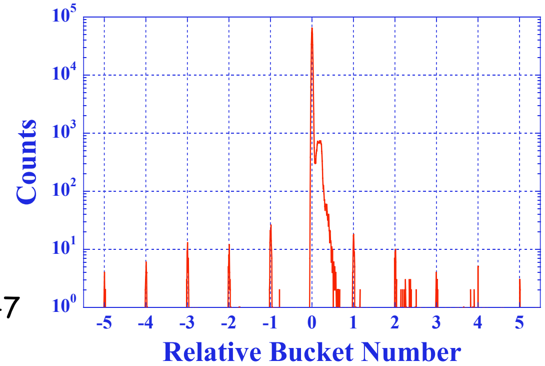

Dynamic Range: $10^{-6} \sim 10^{-7}$

Time to Digital Converter

conventional TAC + MCA (< 1 Mc/s)

FPGA based APS (50 Mc/s)

PicoHarp 300 (10Mc/s)

BESSY II, Diamond, ASP, TLS, SLS ...

http://www.picoquant.com

Gated TCSPC @ SPring-8

Fast Light Shutter

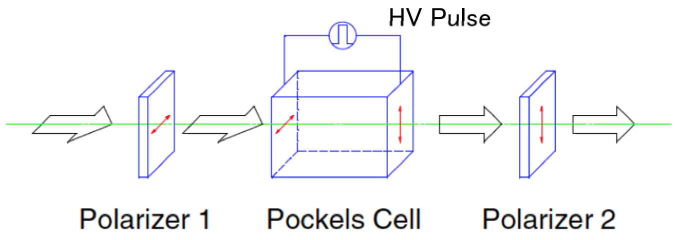

HV Pulser

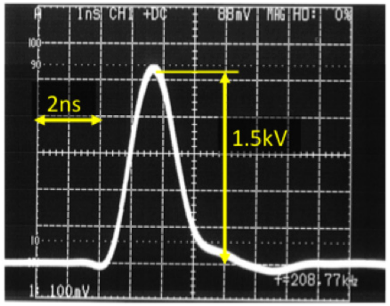

Repetition Rate : 209 kHz (= f_{rev})
Rise/Fall Time: < 2 ns (bunch spacing)
Voltage; 1.5 kV

Measured Time Profile

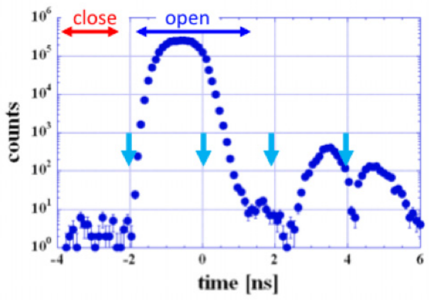

When HV is applied, the polarization is rotated and the shutter is opened.

Gated TCSPC System

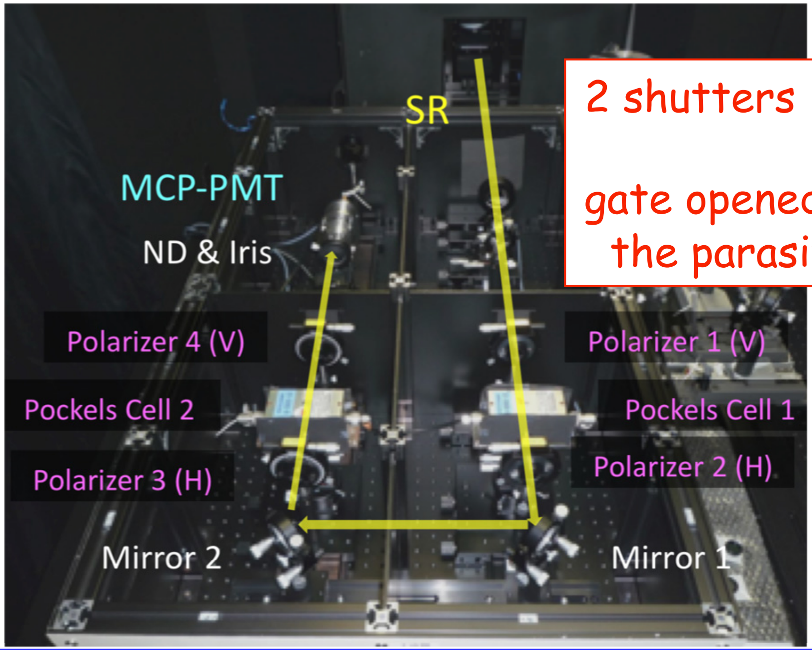

2 shutters in tandem

gate opened to the parasitic bunches

Dynamic Range ~ 10^{-10}

History of the Bunch Purity in FY2009 @ SPring-8

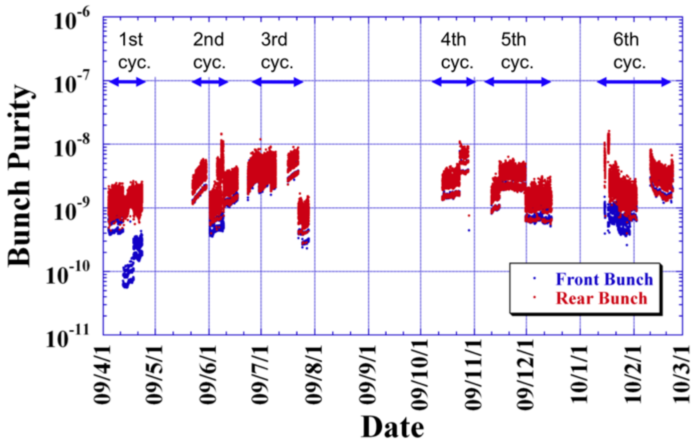

Courtesy of K. Tamura, SPring-8

Diagnostics with a Dedicated Insertion Device (ID)

APS Diagnostic Undulator Line

- Simultaneous measurement of beam divergence and source size
- Horizontal emittance obtained independent of lattice functions

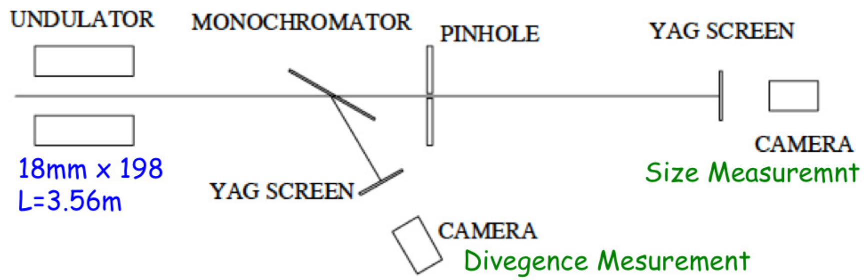

B.X. Yang, A.H. Lumokin, Proc. PAC'99 (1999) p.2161.

ESRF ASD Beamline (ID30)

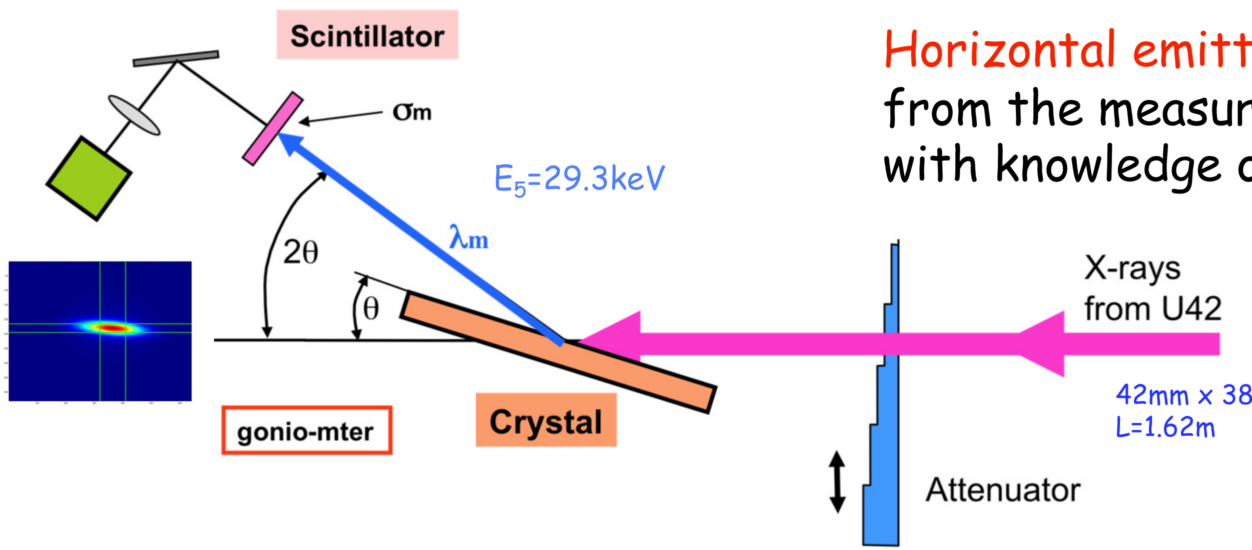

Horizontal emittance is calculated from the measured photon beam size σ_m with knowledge of the lattice parameters.

Courtesy of K. Schedt, ESRF

- Based on the pervious experiment at ID6 beamline
  E. Tarazona, P. Elleaume, Rev. Sci. Instrum. 66 (1995) p.1974.

The SPring-8 Diagnostics Beamline II (BL05SS)

Insertion Device (ID)

Planar Halbach type made of the Ne-Fe-B alloy (NEOMAX-44H)

- Period length: 76mm
- Period number: 51
- Maximum peak field: 0.82T
- Maximum deflection parameter K: 5.8

Energy Spectrum measured at K=5.8

- Rectangular slit aperture on the optical axis : 4.2μrad(H) × 4.2μrad(V)
- Stored beam energy : 8GeV
- Emittance : 3.4nm rad
- Relative energy spread : 0.11%

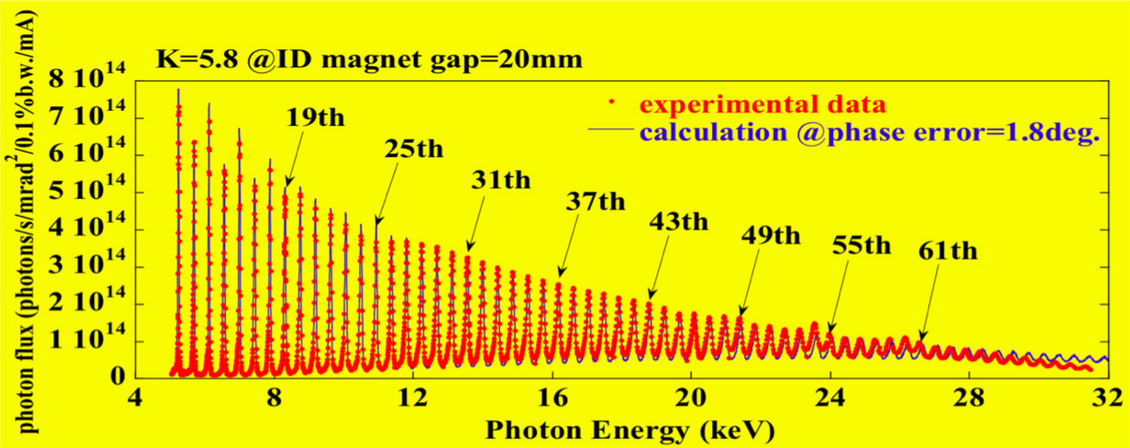

Elaborate tuning of the magnetic field has led to the rms phase error < 2 degrees, which allows us to observe many clear peaks of the higher harmonics.

The measured spectrum is well reproduced by the theoretical calculation assuming the rms phase error of 1.8degree.

Courtesy of M. Masaki, SPring-8

The SPring-8 Diagnostics Beamline II (cont')

Simultaneous Energy Spread & Emittance Measurement

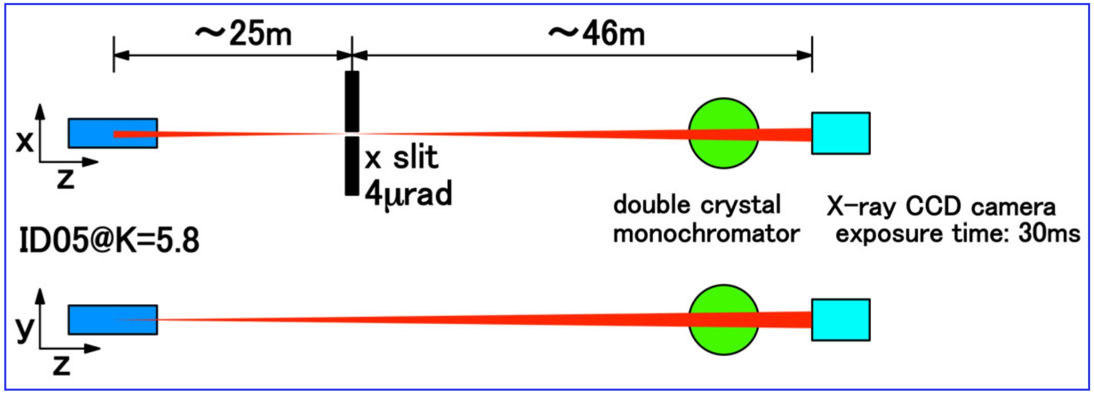

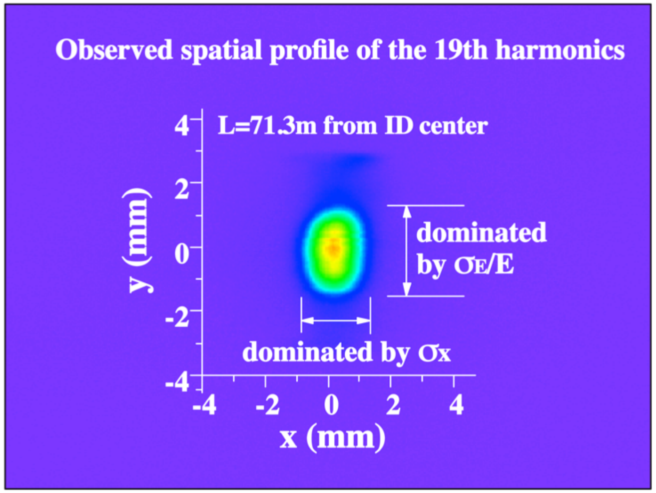

The X slit makes a 1-D pinhole image of the beam in the horizontal

Vertical angular divergence of the photon beam is dominated by the beam energy spread, because of small horizontal-vertical emittance coupling.

Higher harmonics with large K are sensitive to the beam energy spread.

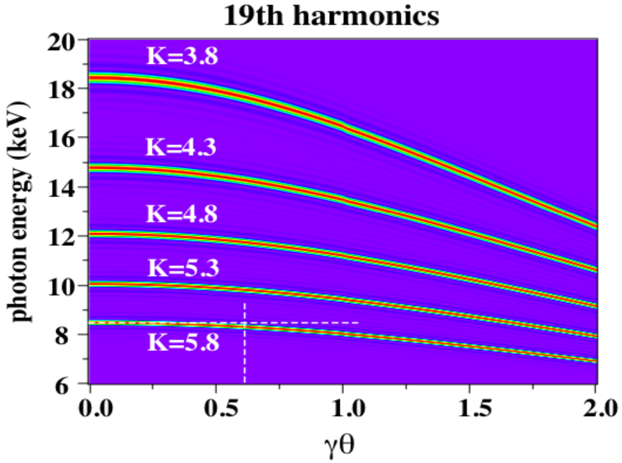

Experimental study of the sensitivity

by modulating RF phase at the synchrotron frequency (~2.2kHz).

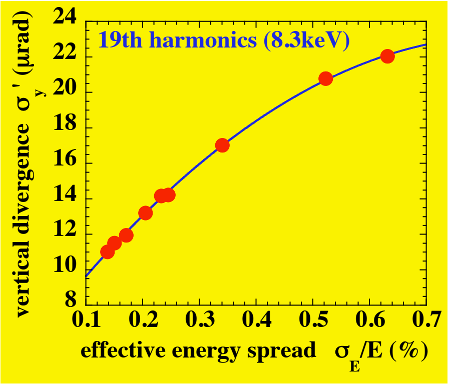

A fast turn-by-turn system under development

Courtesy of M. Masaki, SPring-8

Summary

A brief overview of the transverse beam profiling instrumentation is given.

Bunch length measurements based on the statistical analysis of the intensity fluctuations and on the cross-correlation of the SR and the external laser pulse are described as well as the bunch purity measurement by using a fast light shutter.

Finally, an example of beam diagnostics based on observation of x-rays from a dedicated ID is presented.

Acknowledgements

ALBA: U.Iriso, ALS: F.Sannibale, ASP: M.J.Boland
APS: B.X.Yang, BESSY II: K.Holldack, Diamond: C.Thomas
ESRF: B.K.Scheidt and F.Ewald
NSLS-II: I.Pinayev and P.Ilinski
PETRA III: G.Kube and K.Wittenburg, PF: T.Obina
SPEAR3: J.Corbett, SOLEIL: M.-A.Tordeux and J.-C.Denard
SSRF: K.R.Ye and Y.B.Leng
TLS: C.K.Kuan and T.C.Tseng, UVSOR-II: M. Katoh
SPring-8: M. Masaki and K.Tamura

And Thank You for Your Attention !